

# Chapter 1

## Introduction

### 1.1 Cosmic rays

Cosmic rays are the highly energetic particles (atomic nuclei, electrons, positrons, neutrinos) which are coming from outer space and bombarding our Earth's atmosphere continuously. The extraterrestrial origin of cosmic rays was discovered by Victor Hess [1] in the year 1912 during several ascends with hydrogen-filled balloons up to altitudes of 5 km. But despite many efforts since their discovery more than a hundred years back now, the origin of cosmic rays has been remained one of the central questions of physics and the mechanism which is responsible for the acceleration of cosmic rays at the highest energies is also not totally clear [2]. The energy spectrum of cosmic rays provide some important clues about their origin. The most important feature of the energy spectrum is that it spreads over a wide range of energies, from sub GeV to at least  $3 \times 10^{20}$  eV (the highest energy observed so far). The spectrum can be well represented by a steeply falling power law for energies above the solar modulated one as

$$\frac{dN}{dE} \propto E^{-\gamma} \tag{1.1}$$

where the slope of the energy spectrum changes at least at two points, one around 3 PeV energy where the spectral index steepens from  $-2.7$  to  $-3.1$  (the so called knee of the spectrum) and another around 3 EeV where the spectrum again flattens to pre-knee slope (the so called the ankle of the spectrum) [3]. This two interesting spectral features, Knee and Ankle are supposed to be deeply concerned with the

origin of the cosmic rays. Any viable model of the origin of cosmic rays has to explain all these spectral features of the energy spectrum. Recent observations of Karlsruhe Shower Core and Array Detector-Grande experiment also claim evidence for a second knee around 80 PeV [4, 5] is shown in Fig. 1.1.

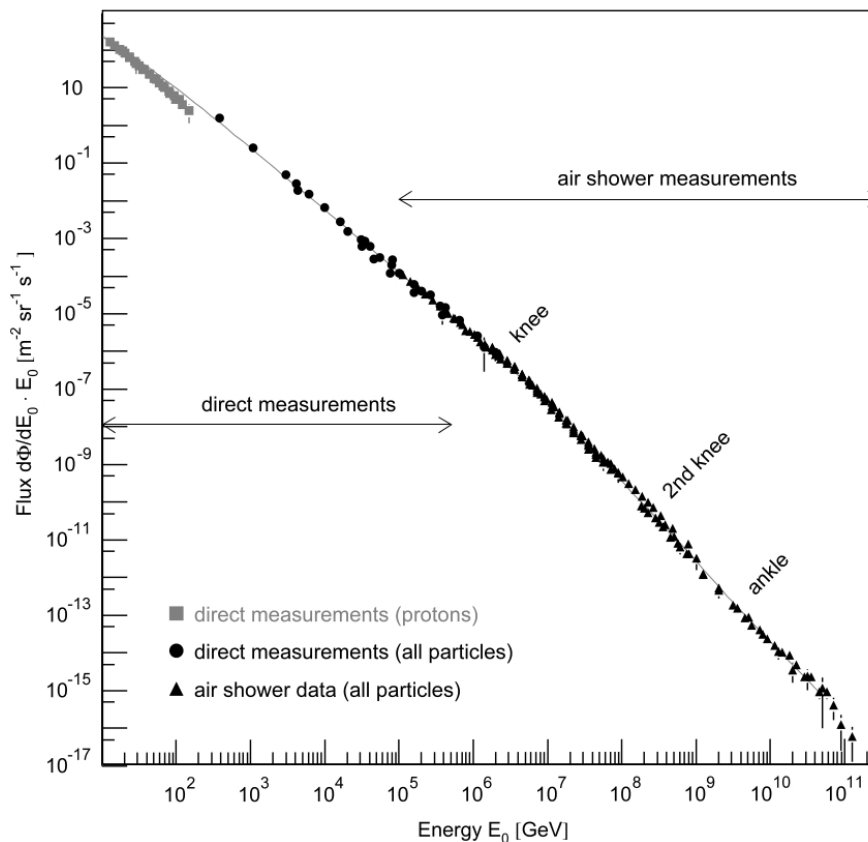


FIGURE 1.1: The differential energy spectrum of primary cosmic rays and its various important features like the  $1_{st}$  knee, the  $2_{nd}$  knee and the ankle (figure taken from [2]).

The primary cosmic rays are studied directly through satellite or balloon borne detectors only up to few hundreds TeV, beyond which direct methods become inefficient due to a sharp decrease in the flux of primary particles. Instead, an indirect method through the observation of cosmic ray extensive air showers (EAS), which are cascades of secondary particles produced by interactions of cosmic ray particles with atmospheric nuclei, has to be adopted [6] for studying cosmic rays above few hundred TeV. But difficulty of this alternate method lies in the reconstruction of the properties of primary cosmic ray particle, such as energy, mass etc.

## 1.2 Origin of Cosmic rays

It is widely believed that bulk of the cosmic rays observed at the Earth, particularly those with energies below the ankle (or below the second knee) are of galactic origin, whereas cosmic rays with energies above the ankle are thought to be of extragalactic origin [7]. The almost uniform power law of the cosmic ray energy spectrum indicates that a unique mechanism is responsible for acceleration of primary cosmic ray particles at all energies, but not necessarily by the same type of source [8]. The first order Fermi acceleration by a relativistic shock front is the most favored model in which a relativistic particle gains energy when it is reflected by the shock front as the shock front is moving towards the particle [9]. The basic principle of acceleration holds good as existing shock fronts in space do not reflect particles instantaneously, but gradually by magnetic fields. Thus, a power law energy spectrum is generated as the particles have a certain probability to escape from the acceleration zone after each reflection at the shock front [8]. The power law index of accelerated cosmic rays is predicted to be around  $-2$  at the source but the spectral index of cosmic rays measured at Earth is found to be  $-2.7$  for  $E \lesssim 10^{15}$  eV [8]. The observed discrepancy in spectral index can be explained by the cosmic ray propagation models for the magnetic fields in the Milky Way and in intergalactic space [10].

The most powerful accelerators of relativistic particles in the Galaxy are believed to be supernovae and supernova remnants, pulsars, neutron stars in close binary systems, and winds of young massive stars on the basis of the cosmic ray energy requirements and the nonthermal radiation as a guideline [11]. Among the Galactic sources, supernova remnants (SNRs) are considered the most viable sources of Galactic cosmic rays below knee of the cosmic ray energy spectrum [7, 12]. Such a proposition has two strong bases: First, the energy released in supernova explosions satisfies the energy requirement to maintain cosmic ray energy density considering an overall efficiency of the conversion of explosion energy into cosmic ray particles of the order of 10% [7]. Second, the diffusive shock acceleration (DSA) operating in SNRs can provide the necessary power law spectral shape of accelerated particles with a spectral index of  $-2.0$  (or slightly less than that) [13] that subsequently steepens to  $-2.7$ , as observed, due to energy-dependent diffusive propagation effects [7].

The situation is more unclear at higher energies as the slope of the cosmic ray energy spectrum steepens at the knee and a majority of the EAS experiments conclude that the knee represents the energy at which proton component exhibits cut-off, which implies that beyond the knee energy, the cosmic ray composition would be heavier, dominated by Fe nuclei [14]. Hence, the knee could represent the maximum energy up to which cosmic ray proton can reach by supernova shock front acceleration. The second knee observed at 80 PeV which is effectively 26 times the energy of the knee, could indicate the maximum energy for iron nuclei ( $Z = 26$ ) reachable in SNR and thus provides additional support to the SNR origin model of cosmic rays [15]. Since the galactic magnetic fields might not be strong enough to bind them anymore at these energies, the leakage of cosmic rays from our Milky Way would be the other explanation for this feature [15]. So at energies beyond 80 PeV, another type of source has to be there for ultra high energy cosmic rays.

According to the theoretical argument by Hillas [16], the maximum energy  $E_{max}$  can be attained by a particle with charge  $Ze$  accelerated in a region with radius  $R$  and magnetic field strength  $B$  is given by

$$E_{max} = \beta Z \left( \frac{B}{1 \mu G} \right) \left( \frac{R}{1 kpc} \right) EeV \quad (1.2)$$

where the velocity of the shock front is  $\beta$  in terms of the speed of light. Hillas [16] had selected several galactic and extra-galactic source candidates of cosmic rays like supernova remnants, neutron stars, gamma ray bursts, and active galactic nuclei and it seems that the ankle of the cosmic ray energy spectrum might be the transition energy from galactic to extra-galactic cosmic rays.

The observed flux of ultra high energy cosmic rays ( $\gtrsim 4 \times 10^{19}$  eV) is consistent with the expected GZK cutoff [17, 18]. The GZK cut-off or rather suppression implies protons with higher energies cannot travel larger distances due to interaction with photons of the cosmic microwave background. The Photo dissociation mechanism [19] for heavier nuclei was proposed as an alternative explanation for the cosmic ray flux at this energy range.

To solve the open question about cosmic ray origin precise and accurate measurements of the flux, energy, arrival direction and particle type (mass) of primary cosmic rays are required.

### 1.3 Gamma ray and Neutrino astronomy

Since cosmic rays are charged particles, they are deflected from their trajectories by the galactic or intergalactic magnetic field. Thus, the arrival direction of Cosmic rays does not point back to their sources and also they are subject to energy loss processes during their propagation [20]. Due to collisions with microwave background photons, the highest energy Cosmic rays ( $E > 5 \times 10^{19}$  eV) are expected to be absorbed. Thus, only Cosmic rays can not provide all information about the inner processes which lead to their acceleration [21].

Primary Cosmic rays are assumed to be accelerated in the different astrophysical sources in the field of high magnetic field or by shock acceleration mechanism. This accelerated Cosmic rays (mainly protons) may interact with the photons in stellar environments and charged and neutral pions are produced via  $\Delta^+$  production through the following channels [22]:

$$p + \gamma \rightarrow \Delta^+ \rightarrow \begin{cases} p + \pi^0 \\ n + \pi^+ \end{cases} \quad (1.3)$$

Primary Cosmic rays may also interact with the ambient matter of the surroundings of the sources, interstellar dust etc. and hence produce charged and neutral pions through the following channels [22]:

$$p + p \rightarrow N[\pi^+ + \pi^- + \pi^0] + X(\text{nucleon}) \quad (1.4)$$

where  $N$  is the pion multiplicity. The charged pions subsequently decay into neutrinos and each neutral pion decay into two gamma ray photons as following [22]:

$$\pi^\pm \rightarrow e^\pm + \nu_e + \nu_\mu + \bar{\nu}_\mu, \quad \pi^0 \rightarrow \gamma + \gamma \quad (1.5)$$

So an alternate approach to search for origin of cosmic rays is the detection of the gamma rays and neutrinos instead of cosmic rays from the probable astrophysical sources in statistically significant numbers.

Our major understanding about the universe comes through photons. The main reason for this is that photons are stable, emitted in large numbers, easy to detect and point back to the source [21]. However, high energy photons above 100 TeV are attenuated by interstellar dust and gas and cosmic background radiation and are not expected to survive from extragalactic distances. But gamma rays can be

originated through leptonic processes as well. Very high energy electrons interact with low energy photons over a wide energy band and can produce high energy gamma photons via inverse Compton scattering [23].

$$e + \gamma_{low} \rightarrow e_{low} + \gamma_{high} \quad (1.6)$$

In the lower energy range, synchrotron radiation processes where electrons lose a fraction of their energy by synchrotron radiation when passing through local magnetic fields, is the dominant production process of gamma rays from leptons. Thus, observations of gamma rays are often equally well described by electromagnetic and hadronic acceleration models, which makes the correlation between gamma rays and cosmic rays unclear.

On the other hand, neutrinos have no electric charge and have a low interaction cross-section with matter. So neutrinos escape unaffected from the inner regions of the most energetic objects seen in the universe and therefore carry crucial information about the nature of the energy-release processes [24]. High-energy neutrinos have only hadronic origin of production and so constitute a direct link between gamma rays and cosmic rays. But all these advantages come with a big disadvantage – cosmic neutrinos are very difficult to detect as they are weakly interacting particles. So immense particle detectors are required to collect cosmic neutrinos in statistically significant numbers [21].

So spectra of gamma-ray emissions can provide only circumstantial evidence for either leptonic or hadronic origin of the gamma rays, while the observation of neutrinos is believed to be a clear proof for hadronic acceleration processes in the source.

## 1.4 Present status of Gamma ray astronomy regarding cosmic ray origin

The theoretical expectations and experimental status of the recent Gamma ray astronomy are discussed below.

### 1.4.1 Theoretical expectations

Among the galactic astrophysical objects, supernova remnants, pulsar and pulsar wind nebula, Binary Systems, Galactic Centre etc. are believed to be violent sources of galactic cosmic rays whereas possible extragalactic cosmic ray sources are active galactic nuclei, gamma ray bursts, Starburst Galaxies etc.

#### Supernova remnants (SNRs) :

A sufficiently massive star undergoes a violent explosion known as a supernova, releasing energy  $\sim 10^{51}$  erg at the end of its life and the outer layers of the progenitor star form the remnant. SNRs are widely believed to be main source of majority of the Galactic cosmic rays, where cosmic rays are accelerated by diffusive shock acceleration (DSA) process in supernova blast waves driven by expanding SNRs [25]. If the cosmic rays are accelerated in SNRs, hadronic interactions of cosmic ray nuclei with the ambient matter/radiation will produce neutral and charged pions which in turn decay into gamma rays and neutrinos respectively. Therefore, SNRs are expected as emitter of TeV gamma rays and neutrinos those are tightly correlated with the primary cosmic rays at the source. The theoretical calculation of Drury et al. [26] and by Naito and Takahara [27] suggest that the luminosity of the nearby SNRs should be sufficient to for detection by the most VHE gamma ray telescopes. For the production spectral index of  $\alpha = 2.1$  of cosmic rays in the SNR, the estimated integral gamma ray flux of energy above 1 TeV at the Earth [26] is given by

$$F(> E \text{ TeV}) \approx 9 \times 10^{-11} \left( \frac{E}{1 \text{ TeV}} \right)^{-1} \left( \frac{\xi E_{SN}}{10^{51} \text{ erg}} \right) \left( \frac{r}{1 \text{ kpc}} \right)^{-2} \left( \frac{n}{1 \text{ cm}^{-3}} \right) \text{ cm}^{-2} \text{ s}^{-1} \quad (1.7)$$

where  $r$  is the distance of SNR from earth,  $\xi$  is the fraction/efficiency of the total energy of the supernova explosion  $E_{SN}$  transferred to the cosmic ray particles and  $n$  is the average ambient matter density around the remnant. The energies above 100 MeV (close to the COS-B threshold energy and within the EGRET range), the flux of gamma rays from a SNR is thus given by [26]

$$F(\geq 100 \text{ MeV}) \approx 4.4 \times 10^{-7} \left( \frac{E}{1 \text{ TeV}} \right)^{-1} \left( \frac{\xi E_{SN}}{10^{51} \text{ erg}} \right) \left( \frac{r}{1 \text{ kpc}} \right)^{-2} \left( \frac{n}{1 \text{ cm}^{-3}} \right) \text{ cm}^{-2} \text{ s}^{-1} \quad (1.8)$$

where the efficiency  $\xi$  for converting the kinetic energy of the SNR explosions into cosmic rays is required to have a value of  $\sim 10\%$  to satisfy the power budget of the galactic cosmic rays [26] but it is found to be uncertain for different SNRs.

**Pulsars and Pulsar Wind Nebulae (PWNe) :**

Pulsars are rapidly rotating highly magnetized neutron stars, formed after a SN explosion, where rotation axis is misaligned with magnetic field axis. The Pulsars can drive powerful winds of highly relativistic particles to form a nebula called pulsar wind nebula and they are often found inside the shells of supernova remnants in their early stages of evolution. Pulsars and PWNe are the another important probable sources of galactic cosmic rays. Several detailed mechanisms including the popular polar gap [28], the outer gap [29] and the slot-gap model [30, 31] have been proposed so far for acceleration of particles by pulsars. Link & Burgio (2005) [32] inferred that protons or heavier ions are accelerated to PeV energies near the surface of a pulsar by the polar caps when  $\mu\Omega < 0$  where  $\Omega$  is the angular velocity and  $\mu$  is the stellar magnetic moment of the pulsar. When pulsar accelerated ions interact with the thermal radiation field of pulsar, both charged and neutral pions are produced and subsequent decay of them will lead to emission of high energy neutrinos and gamma rays simultaneously [33]. Thus, the phase-averaged flux of gamma rays and neutrinos reaching at earth from the pulsar of distance  $d$  is given by [32, 33]

$$\phi = 2c\xi\zeta\eta f_b f_d (1 - f_d) n_0 \left(\frac{R}{d}\right)^2 P_c \quad (1.9)$$

where  $f_b$  denotes the duty cycle of the gamma-ray/neutrino beam,  $\xi$  is 4/3 and 2/3 for gamma-rays and muon neutrinos, respectively,  $\zeta$  represents the effect due to neutrino oscillation with values  $\zeta = 1$  and 1/2 for gamma-rays and muon neutrinos, respectively,  $n_0$  is the Goldreich–Julian density [34] of ions at radial distance  $r$  from pulsar,  $f_d$  is the depletion factor of polar gap of pulsar and  $R$  is the stellar radius.

**Active Galactic Nuclei (AGN) :**

Active Galactic Nuclei (AGNs) are the distant galaxies with bright nuclei which is powered by in-falling material toward a supermassive black hole from host galaxy. A rich phenomenology of AGNs can be observed leading to many classes and subclasses as Blazar, Quasar, Seyfert, Radiogalaxy depending on the observation angle with respect to the jet axis [35]. For gamma-ray astronomy, the most important ones are Blazars, which include BL Lacertae objects (BL Lacs) and flat-spectrum radio quasar (FSRQs), whose jets points directly in the direction of the Earth [35].

AGN jets are one of the prime candidate sources of extragalactic cosmic rays which can accelerate cosmic rays with energy spectra extending beyond  $10^{20}$  eV [36]. The leptonic models of blazars assumes that synchrotron and inverse Compton (IC) radiation of the directly accelerated electrons in the relativistic jets generates low energy and high energy hump in gamma ray energy spectra [37]. The most widely accepted and popular emission model of gamma rays for blazars like Mkn 421 is the Synchrotron Self Compton (SSC) specially at TeV energies. In the SSC model, the energetic electrons interact with the magnetic field to emit synchrotron emission and the same population of electrons up-scatter by IC scattering this low energy synchrotron photons within the jet [38]. The high energy hump in gamma ray spectrum may also be produced according to External Compton (EC) model, i.e via IC scattering of electrons with external photon fields from the optical-UV emission from the accretion disk and the infrared (IR) radiation field produced by the torus or from the broad line region (BLR) of AGN [39]. The hadronic models, so called proton-induced cascade model [40] suggest that accelerated hadronic matter and protons in AGN jets may interact with the low energy synchrotron photons via photo-pion interactions and subsequently produce TeV gamma rays by decay of neutral pions [41]. The high energy hadronic component contributes to the high-energy bump of gamma ray spectra of AGN. Protheroe and Kazanas in 1983 [42] had presented a hadronic model of gamma ray emission with main features and predictions for a class of quasars and active galactic nuclei like 3C273. In the model of Atoyan and Dermer [43], the fluxes of high-energy neutrinos and gamma-rays from the FSRQ blazar 3C279 and BL Lac object Mkn 501 produced in hadronic interaction are estimated considering that the power to accelerate relativistic protons is equal to the power injected into relativistic electrons needed to explain the non-thermal flares detected by EGRET [44].

### **Gamma Ray Bursts (GRBs) :**

Gamma-ray bursts (GRBs) are most violent phenomena of gamma ray emission which generally appear to last for milliseconds up to seconds and come at random times and from random directions in the sky. GRBs are believed to originate from merging compact objects (such as neutron stars or black holes) or collapsing massive stars, and are associated with the formation of black holes [45]. GRBs are potential extragalactic sources of the observed ultra-high-energy cosmic rays where internal shocks may allow cosmic ray nuclei to achieve maximum energies  $\gtrsim 10^{20}$  eV [46]. In the general fireball model scenario [47], both leptonic and hadronic models are predicted as the possible High Energy (HE) and Very High

Energy (VHE) emission mechanisms from GRBs. In the leptonic models, gamma ray spectrum in the 10 KeV to 1 MeV energy band in  $\sim 2/3$  of bursts can be explained with synchrotron emission [48] and gamma ray emission in GeV band can be explained in terms of inverse Compton (IC) scattering by relativistic electrons. According to the Synchrotron Self-Compton (SSC) models [49], correlated HE and Low Energy (LE) emission is expected as relativistic electrons are scattered by the soft photons which produced in synchrotron radiation by the same electron. In a hadronic environment [50], relativistic protons interact with the  $\sim 100$  KeV burst photons producing neutral pions which immediately decay into high energy gamma-rays. There are many other hadronic cascade models have been proposed, i.e. high energy emission from proton-synchrotron and photo-meson cascade emission in internal shocks [51, 52]; proton-neutron inelastic collisions early in the evolution of the fireball [53]. Dermer & Atoyan 2004 [54] invoked a hadronic model to explain the additional spectral component observed in GRB 941017 and predicted to peak in the MeV to GeV band [51] which would produce a clear signal in the LAT energy band. The Cannonball model (CB) [55] predicts narrow GeV emission flares from pion decay which arriving about 1 second earlier than the GRB emission and each pion decay are associated with one of the CBs. According to the Compton drag model [56], the surrounding plasma is so dense that it opaque to the energetic photons (self-absorbed via  $\gamma + \gamma = e^+ + e^-$ ) when the GRB is radiated and hence the model predicts no GeV gamma radiation at all.

### 1.4.2 Experiments

The atmosphere being opaque to photons beyond the optical waveband from reaching the Earth surface, making it impossible to detect gamma ray emission directly. In the high-energy (HE) domain, direct detection of gamma ray requires space-based experiments. At higher energies above 100 GeV, a ground-based technique is needed as the detection area of space-based detectors is not sufficient. The operating principle of the Ground-based instruments is to detect the secondary products of the interaction between gamma rays and the atmosphere.

### 1.4.2.1 Space based High-energy gamma ray astronomy

Due to the high level of secondary gamma rays produced by cosmic rays in the atmosphere, the first attempts to detect cosmic gamma rays with balloon-borne detectors were unsuccessful. The Explorer-11 [57] and OSO-3 [58] satellites in 1961 and 1968, respectively were the space based detectors which were successful to detect high energy cosmic gamma rays above 50 MeV for the first time. A total of 31 and 621 cosmic gamma rays were discovered by Explorer-11 and OSO-3 respectively. The OSO-3 satellite provided the first clear evidence for gamma ray emission from the Milky Way [58]. In 1967, the discovery of cosmic gamma ray bursts, or GRBs was made by the network of Vela satellites from the United States Department of Defense, which were designed to monitor nuclear tests in the atmosphere after the signature of the Nuclear Test Ban Treaty in 1963 [59]. The astronomical community declassified the discovery and publicized in 1973 as a new class of astronomical phenomena whose origin is remained as a puzzle till now. In the 1970s, The two satellite COS-B [60] and SAS-2 [61] operated in the 35 MeV-5 GeV energy range are the following space missions which provided clear evidence for the first significant gamma ray detection. The major step forward in gamma-ray astronomy is that the SAS-2 satellite detected the diffuse emission concentrated along the galactic plane, discovered the Crab and Vela nebulae and the periodic signals from their pulsars [61]. On the other hand a catalog of 25 galactic sources except one extragalactic source, the quasar 3C273 were produced by COS-B satellite [60].

The gamma ray astronomy has become an integral part of astronomy during nine years of mission in orbit of Compton Gamma-Ray Observatory (CGRO) [62], launched in 1991 with four gamma-ray instruments on board which were the Energetic Gamma Ray Experiment Telescope (EGRET) for energies above 30 MeV, the gamma-ray Burst and Transient Source Experiment (BATSE), the Compton Telescope (COMPTEL) for the energy range 1-30 MeV and the Orientation Scintillation Spectrometer Experiment (OSSE). The CGRO [62] Telescope revealed the different variety of sources emitting gamma rays are present in the universe, such as the Sun, isolated spin-down pulsars, accreting binaries with stellar neutron stars and black holes, supernovae and supernova remnants, the interstellar medium, normal and radio galaxies, Seyfert galaxies, gamma ray bursts and quasars.

The Fermi gamma ray space telescope (Fermi) [63], launched on 11 June 2008, is currently surveying the sky in the GeV energy range with unprecedented sensitivity and angular resolution. The primary instrument of Fermi telescope is the Large Area Telescope (LAT) which is a wide field-of-view pair-conversion telescope covering the energy range from 20 MeV to more than 300 GeV. Another instrument on board of Fermi is the Gamma-ray Burst Monitor (GBM) which complements the LAT in its observations of transient sources and is sensitive to x-rays and gamma rays with energies between 8 KeV and 40 MeV. Since operating in space, Fermi-LAT has significantly improved our understanding of the MeV to GeV gamma ray sky. Till now the Fermi LAT has observed a large number of sources that include active galaxies (more than 1200 by now), pulsars, compact binaries, globular clusters, supernova remnants etc [64]. More recently, the Fermi-LAT observed a large sample of infrared luminous galaxies, detecting two additional starburst galaxies at GeVs, NGC 1068 and NGC 4945 [65]. The prolonged high energy  $\gamma$ -emissions in solar flares have been detected by the EGRET telescope on board the Compton gamma ray observatory [66] and the Large Area Telescope (LAT) on board the Fermi Gamma-Ray Space Telescope (Fermi) [67, 68] which are believed to be originated from the  $\pi^0$  decay and thereby an evidence of particle acceleration in solar flare [67, 68]. The Fermi-LAT community publish Second Source Catalog [63] 2FGL which contains 1873 sources including various classes of objects, and a third catalog has also recently been published [69]. The Italian gamma ray satellite, AGILE have also contributed important results. The spectacular progress of space-based gamma ray astronomy at high energies in the last more than 35 years are summarized in Table 1.1

TABLE 1.1: Space experiment catalogs of sources in high-energy gamma ray astronomy.

Satellite or experiment	Catalogue	Year of the catalog	Number of sources
COS-B	2CG [60]	1981	25
EGRET	3EG [70]	1999	271
Fermi LAT	2FGL [63]	2012	1873
Fermi LAT	3FGL [69]	2015	3033

### 1.4.2.2 Ground based High-energy gamma ray astronomy

Above 30 GeV energy, the gamma-ray fluxes from cosmic astrophysical sources becomes very low so that Satellite-borne detectors like Agile, Fermi and Integral detectors cannot collect a statistically significant number of events in a reasonable amount of time [71]. Very high energy gamma rays interact with atmospheric nuclei while impinging on the Earth and usually producing an electron-positron pair which in turn initiate a large particle cascade via Bremsstrahlung and further pair-production, leading to the formation of an extensive air shower (EAS) detectable from the ground. An indirect approach which images the EAS to derive the direction and energy of the primary gamma ray photon is the Ground-based gamma-ray astronomy. There are basically two classes of Ground-based gamma-ray telescopes: one is observing the Cherenkov light that is produced by the secondary particles in the shower and other is the direct detection of the secondary particles of EAS [64].

The most efficient techniques or telescopes now a day to study gamma-ray induced atmospheric Cherenkov light is the Imaging Air Cherenkov Telescopes (IACT) composed of up to several 100 m<sup>2</sup> large optical mirrors and photo-multiplier tube based cameras with hundreds to thousands of pixels, as they provide excellent angular resolution ( $< 0.1^\circ$ ) together with strong background rejection power ( $> 99\%$ ) [72]. But the relatively low duty cycles ( $\sim 10\%$ ) and narrow fields of view ( $\sim 5^\circ$ ) are the drawbacks of IACTs [72]. The Whipple telescope, HEGRA, CAT and more recently, H.E.S.S., VERITAS and MAGIC are the well known examples of IACTs.

The Whipple Observatory [73] was the first Imaging Air Cherenkov Telescopes (IACT) having 10 meter gamma-ray telescopes in Arizona, which saw its first light in 1968. A major success of this observatory is the detection of the Crab Nebula at VHE gamma rays for the first time, in 1989 [73].

**H.E.S.S.** (High Energy Stereoscopic System) [74] is an array which consists of four 100 m<sup>2</sup> Cherenkov telescopes located in the Khomas Highlands of Namibia at 1800 m above sea level and sensitive to the faint flashes of Cherenkov light emitted in extensive air showers created by cosmic rays or gamma rays [75]. The initial four HESS telescopes are located on a square with a 120 m side length. In the phase-II of the project, a considerably larger telescope of 600 m<sup>2</sup> surface area was added at the center of the array which increases the energy coverage, sensitivity

and angular resolution of the instrument. The H.E.S.S. observatory is located in the southern hemisphere which allows it to observe major parts of the Milky Way including the Galactic Center. HESS is sensitive to detect point sources with a flux of 0.7% of the Crab nebula in a 25-hour exposure at the  $5\sigma$  significance level [23].

**VARITUS** (Very Energetic Radiation Imaging Telescope Array System) [76] is an array which consists of four 12 m telescopes located at the Fred Lawrence Whipple Observatory (FLWO) in southern Arizona. VARITUS has an effective area of approximately  $10^5 \text{ m}^2$  and sensitive to gamma rays in the energy range from 85 GeV to 30 TeV with energy resolution 15 – 25%. The overall sensitivity of the array is increased about 30% when one of the four telescopes of the array was relocated to a different position in 2009. Currently it has a sensitivity to detect a 1% Crab source with a  $\sim 25$  hours exposure [77]. Since 2007, more than 20 extra-galactic objects has been detected by VARITUS. In recent years its focus has shifted to long-term monitoring of known sources rather than discovery of new targets [23].

**MAGIC** (Major Atmospheric Gamma Imaging Cherenkov) [78] telescopes consists of a system of two 17 m diameter IACTs located at La Palma on the Canaries Island at an altitude of 2200 m and observing since 2004. The sensitivity has been improved by a factor of two at the energy threshold of 70 GeV by the recent upgrade of the camera and trigger system. The system provides an integral sensitivity of  $0.71 \pm 0.02\%$  of the Crab Nebula flux for a 50-hour observation and performing well [23]. The telescopes are made lightweight which enables fast slewing of the telescope so as to rapidly follow up on alerts to gamma ray bursts (GRBs). MAGIC collaboration observed VHE gamma rays from SNR IC 443 for a total of 10 hours in the period December 2005 to January 2006, with the telescope pointing to the SNR center [79].

**CTA** (Cherenkov Telescope Array) [80] is planned to be the next generation ground based IACT observatory that builds on the success and experience gained from current IACTs (i.e. H.E.S.S., MAGIC and VERITAS) for very high energy (VHE) gamma-ray astronomy. The CTA observatory consists of two IACT arrays, one in the northern and one in the southern hemisphere to provide all-sky coverage. More than a hundred IACTs of three different size classes are equipped to cover the energy range 20 GeV to 300 TeV, one is large sized telescopes (LSTs)

for energies from the threshold to a few 100 GeV, second is medium-sized telescopes (MSTs) for the core energy range 100 GeV to 10 TeV and third class is small sized telescopes (SSTs) for high energies above a few TeV [71, 72]. CTA will reach 1 mCrab for a typical observing time of 50 h as its sensitivity will be a factor of 10 more than any existing VHE instrument [81]. CTA will cover four orders of magnitude in energy which is again a factor 10 more than any existing facility. CTA can reach angular resolutions of better than  $2''$  for energies  $>1$  TeV by selecting a subset of gamma-ray induced cascades detected simultaneously by many of its telescopes [72]. The observatory, CTA will provide an unprecedented census of VHE source population in the Universe by performing deep surveys of the Galactic plane and the extragalactic space down to a uniform sensitivity of a few mCrab.

**HAWC** (High-Altitude Water Cherenkov observatory) [72], a direct successor to the MILAGRO instrument [82] spread over 20000 m<sup>2</sup> on a 4100 m plateau near the Sierra Negra, Mexico. It is optimized for reconstructing gamma-ray air showers can provide observations of TeV gamma-rays with a high duty cycle and wide field of view. HAWC is essentially at an altitude above 4000 m, which results in a 15-fold increase in gamma-ray sensitivity and a lower energy threshold  $\sim 100$  GeV [83]. Since beginning of 2015, HAWC is fully deployed of 300 cylindrical water Cherenkov detector (WCDs) of 7.3 m diameter and 4.5 m height which are filled with clear water and instrumented each with four upward facing photo-multiplier tubes (PMTs) [84]. HAWC has an instantaneous field of view of about 1.8 sr. due to its aperture of  $< 45^\circ$  in zenith angle. Within one year of observations, a source detection sensitivity above 2 TeV of HAWC will reach nearly 50 mCrab for a good fraction of the observable sky [84]. The lifetime of the observatory is expected to be 10 years.

**LHAASO** (Large High Altitude Air Shower Observatory) [72, 85] which will be located at Daocheng (China) at an altitude of 4300 m, is a planned experiment for gamma-ray and cosmic-ray physics. Being a hybrid detector array, LHAASO will be composed of a 90000 m<sup>2</sup> large water Cherenkov detector array (WCDA), a 1 km<sup>2</sup> large detector array (KM2A), 24 wide field Cherenkov telescopes (WFCTA), and a 5000 m<sup>2</sup> large array of shower core detectors (SCDA) [72]. The detectors, WFCTA and SCDA aim at the detection of cosmic rays above 30 TeV whereas WCDA and KM2A will detect gamma rays in the 0.1 – 1000 TeV energy range. WCDA and KM2A have an instantaneous field of view of 1.5 sr. due to an aperture

of  $< 40^\circ$  in zenith angle [72]. LHAASO provides thus a daily sky coverage of 7 sr. which corresponding to roughly half of the sky as the location of the observatory at  $29^\circ$  northern latitude. Depending on declination, most of the sources are visible for 4-6 hours during one day [72]. The experiment is expected to become operational in the 2020.

### 1.4.3 Observational results

The last decade has shown that high energy gamma-ray emission occurs in many different kinds of sources.

#### Supernova Remnants (SNRs) :

In the TeV domain, presently about sixteen shell-type SNRs have been firmly identified as VHE gamma-ray emitters as shown in table 1.2.

TABLE 1.2: Firmly detected Shell-like SNRs at TeV energies [86].

Name	Dist (kpc)	Flux(Crab Units)	Discovery (year)
SN 1006	2.18	-	CANGAROO (1998)
RX J1713.7-3946	1	0.66	CANGAROO (2000)
Cassiopeia A	3.4	0.03	HEGRA (2001)
RX J0852.0-4622	0.2	1	CANGAROO (2005)
HESS J1614-518	-	0.25	H.E.S.S. (2005)
CTB 37B	13.2	0.018	H.E.S.S. (2006)
IC 443	1.5	0.03	MAGIC (2007)
HESS J1731-347	3.2	-	H.E.S.S. (2007)
HESS J1912+101	-	0.1	H.E.S.S. (2008)
RCW 86	2.5	0.1	H.E.S.S. (2008)
SN 1006 SW	2.2	0.01	H.E.S.S. (2008)
SN 1006 NE	2.2	0.01	H.E.S.S. (2008)
0FGL J1954.4+2838	9.2	0.23	Milagro (2009)
SNR G106.3+02.7	0.8	0.05	VERITAS (2009)
Tycho	3.5	0.009	VERITAS (2010)
HESS J1534-571	-	-	H.E.S.S. (2015)

The collaboration of CANGAROO observatory in 1998 [87, 88] reported the first detection of TeV gamma-ray emission from the RX J1713.7 – 3946 SNR, and it was confirmed by the subsequent observations with CANGAROO-II in 2000 and 2001 [89]. The HESS Collaboration also obtained a resolved image of the source in TeV gamma rays [90]. The TeV gamma rays from SNR RX J1713.7 – 3946, one of the most prominent examples of TeV-emitting SNRs, can be explained by a

hadronic scenario i.e. the decay of  $\pi^0$  mesons produced in pp collisions [91] if the average magnetic field strength is larger than  $15 \mu\text{G}$  [92]. The CANGAROO and H.E.S.S. collaboration also reported the detection of non-thermal TeV gamma rays from the SNR RX J0852.0 – 4622 (also known as G266.2 – 1.2 or Vela Jr.) [93]. The high energy gamma ray emission from RX J0852.0 – 4622, a nearby SNR, can be explained either by a leptonic scenario (i.e, inverse Compton scattering by electrons) or by a hadronic scenario [94]. The SNR Cassiopeia A has been observed by Fermi-LAT [95] in GeV energies, whereas the HEGRA [96], MAGIC [97], and VERITAS [98] telescopes detected the source at TeV energies. The observed GeV–TeV gamma-ray spectrum from Cas A can be explained by hadronic interactions of cosmic rays with the ambient (proton) matter, when a power-law spectrum of protons with a power law index 2.3 is considered and the maximum energy of cosmic ray protons is taken as 100 TeV [95]. Fermi has observed SNR Tycho in the GeV energies [99], whereas the VERITAS Collaboration observed the source in the 1–10 TeV range. The observed overall gamma-ray spectrum of Tycho is found to be consistent with the early theoretical predictions [26]. A single power law with a photon index of 2.1–2.2 can describe the GeV–TeV energy spectrum well [100, 101]. So the gamma-ray observations in the TeV range provide direct support for the acceleration of particles up to nearly 100 TeV or more in SNR shells [102].

Gamma rays of GeV energies from some SNRs interacting with molecular clouds such as W51C [103], W44 [104, 105], IC 443 [106, 107] and W28 [108–110] have been observed by the Large Area Telescope (LAT) on board the Fermi Gamma-ray Space Telescope and the Gamma-Ray Image Detector (GRID) on board AGILE satellite. The current generation of imaging atmospheric Cherenkov telescopes have also detected the systems in the TeV energy range [108]. Observation of TeV gamma rays from the molecular cloud instead of directly from SNR provide strong support to a hadronic origin of the gamma-ray emission [105]. The characteristic spectral feature of gamma ray emission detected from W44 [105] and IC443 [111] are recently explained the decay of  $\pi^0$  produced in hadronic-induced interaction with the molecular clouds. Another clean signature for the hadronic acceleration in supernovae will be the observation of TeV neutrinos from SNRs. Again a clear signature of gamma rays originating from pion decay ( $\pi^0 \rightarrow 2\gamma$ ) should be a gamma-ray emission spectrum that peaks at 67.5 MeV, and evidence for a cut-off below several hundreds of MeV from some SNRs has already been found by AGILE and Fermi [111].

**Pulsars and Pulsar Wind Nebulae (PWNe) :**

Pulsars and PWNe are found to be a prominent source in the gamma-ray sky since the birth of gamma-ray astronomy and about 37 PWNe have been detected in TeV gamma rays so far [86]. The Crab along with its associated Nebula was the first pulsar detected at TeV energies by Whipple 10m observatory [73]. Crab Nebula is powered by the strongly magnetized wind of the Crab pulsar and it now serves as the standard candle of TeV astronomy. The VERITAS and MAGIC collaborations [112, 113] detected pulsed emission above 100 GeV from the pulsar in the Crab Nebula, favouring models with exponential or sub-exponential cut-offs (slot gap and outer gap models). Recently MAGIC [114] observed a pulsed emission from the Crab above 400 GeV that extends beyond TeV energies, challenges the theoretical models. This emission can be explained by different current models such as secondary emission of electrons in the outer magnetosphere [115] or IC emission from energetic electrons in the ultra-relativistic pulsar wind [116]. Recently H.E.S.S. collaboration announced a detection of pulsed emission down to energies of 20 GeV from a pulsar, Vela [117]. To explain the emission from Crab, Vela and millisecond pulsars, synchrotron self-compton emission from pairs was proposed recently [118]. To reproduce the gamma rays spectrum from Crab and Vela X respectively, hadronic models have been used and show that noticeable contribution of this gamma rays may be expected only at energies above 10 TeV [119, 120]. So far no information is found related to the acceleration of relativistic protons in the pulsar. The Fermi-LAT collaboration first reported the pulsed gamma ray emission above 25 GeV from another pulsar, Geminga which rules out the polar-cap model in which a super-exponential cut-off is expected at a few GeV energy [121]. Recently the VERITAS collaboration reported that no signal was detected above 100 GeV from the Geminga pulsar [122]. At TeV energies, an extended steady emission from Geminga at a significance of  $6.3\sigma$  was reported by the Milagro collaboration and recently confirmed by HAWC [123]. Recently, VERITAS observatory discovered the TeV emission from G54.1 + 0.3, a Pulsar Wind Nebula (PWNe) [124] presents a brand new event for highlighting the relative significance of hadrons in PWNe.

**Active Galactic Nuclei (AGN) :**

Most of the AGN which were detected by the EGRET telescope of the Compton Gamma-Ray Observatory, are identified with blazars, a subset of radio-loud AGN for which the jet is pointed toward Earth [70, 125]. Using the first four years of the Fermi-LAT data with the high-confidence clean sample, the Third Large

Area Telescope Catalog of Active Galactic Nuclei (3LAC, published in 2015) [126] includes 1444 gamma-ray AGNs, comprising 604 BL Lac objects ( $\sim 40\%$ ), 404 FSRQs ( $\sim 30\%$ ), 402 blazars of unknown type ( $\sim 30\%$ ), and 24 non-blazar AGNs ( $\sim 2\%$ , which are mainly radio galaxies, radio-loud narrow line Seyfert galaxies, and candidate Seyfert AGN). The Fermi LAT sees primarily blazars which indicates that relativistic jets with strong Doppler boosting are dominant sites of extragalactic gamma ray production.

At TeV energies, Ground-based first-generation telescopes like Whipple 10-m Telescope, HEGRA and CANGAROO detected a few AGNs such as the first detected blazar Mkn 421 [127], Mkn 501 [128] and PKS 2155–304 [129]. Ground-based gamma-ray instruments now detected more than 60 AGNs at very high energy gamma rays including BL Lacs and FSRQs [86]. Several explanations based on hadronic [40, 130, 131] and leptonic origin [38, 132, 133] of gamma rays have been proposed for the formation of the spectrum of these objects. Recently current generation ground based detectors detected VHE  $\gamma$ -ray emission from luminous Flat Spectrum Radio Quasars (FSRQs)-type blazars which includes PKS 1510–089 by HESS [134], 3C 279 by MAGIC [135], PKS 1222+216 by MAGIC [136], and S3 0218+35 [137], also the very recent detection of PKS 1441+25 by VERITAS [138] and by MAGIC [139]. Currently three radio galaxies such as the M87 [140–142], Centaurus A [143], and NGC 1275 [144] have been confirmed to exhibit TeV emission.

### **Gamma Ray Bursts (GRBs) :**

GRBs are observed as one of the most luminous extragalactic phenomena in gamma ray sky. Observations at higher energies above 30 MeV were first made from seven GRBs with the EGRET Telescope on board the CGRO satellite [145, 146]. The MeV emission from most detected GRBs is consistent with being a continuation of the GRB spectra at lower energies and does not show any indication of a cut-off [147]. However, high energy gamma ray emission from one GRB exhibited an additional hard power-law component, which challenges the synchrotron model interpretation of radiation from charged particles [148]. One of the important bursts was GRB 940217 as a gamma ray photon of 18 GeV energy was detected from the bursts 90 minutes after the prompt emission and the emission might have lasted more than 5000 s which indicates a temporally-extended emission from GRBs [149]. Recently Fermi-LAT observes a subset of GRBs at high energy gamma rays and thus allowing more detailed studies [146]. The gamma ray

emission is found to be consistent with a Band function from keV to GeV energies from some GRBs e.g, GRB 080916C [150], whereas some other bursts exhibit an additional hard power-law component at high energy like GRB 090902B & 090510 [150, 151], which in some cases shows a spectral break like GRB 090926A [152]. Fermi-LAT finds that the gamma ray emission from GRBs above 100 MeV starts systematically later than the emission at lower energies e.g., delays up to 40 s is reached for GRB 090626 [153]. Fermi-LAT recently detected a highest energy of 95 GeV photon a few minutes after the burst began and a 32 GeV photon after more than 9 hours after burst start from GRB 130427A at redshift  $z = 0.34$  [45]. Additionally, the observations of high energy emission from the GRB which lasted for 20 h, are not in agreement with being synchrotron radiation in the standard afterglow shock model [45]. So inverse Compton radiation from the external shocks [154] can be an alternative scenario for non-thermal photons at GeV energies.

According to the framework of the fireball model, GRBs are predicted to emit very-high gamma rays with  $> 100$  GeV energy and extending observations of GRBs at this energy region are required to further study the acceleration and radiation processes at work (e.g. an inverse Compton scenario has been proposed for GRB 130427A [155]). The Milagrito experiment [156] claimed to have observed emission from GRB 970417A at about 0.1 TeV energy photon at a  $\sim 3\sigma$  significance but its successor, Milagro did not find any significant signal in more than 50 GRBs observed. Being sensitive in this energy range ( $> 100$  GeV), different Imaging Atmospheric Cherenkov Telescopes (IACTs) routinely look for TeV emission from GRBs, but only upper limits on the very high energy emission have been reported so far [157–160].

## 1.5 Current status of Neutrino astronomy regarding cosmic ray origin

High energy gamma ray detection from any source is significant but not sufficient evidence for hadronic acceleration of cosmic rays in that source. Instead observation of TeV neutrinos from astrophysical sources is supposed to provide a clean signature for the hadronic acceleration at the source. The theoretical expectations and observational status of the Neutrino astronomy concerning origin of hadronic cosmic rays are discussed below.

### 1.5.1 Theoretical status

**SNRs** are predicted to be one of the prime candidates for GeV–TeV energy neutrino production, typically via decay of charged pions produced in the proton–nucleon collisions if cosmic rays are accelerated at their shock front. The estimated integral neutrino flux from a SNR of energy above 1 TeV at the Earth [161] is given by

$$F_{\nu_\mu}(> 1 \text{ TeV}) \approx 3.4 \times 10^{-11} \left( \frac{E}{1 \text{ TeV}} \right)^{-1.2} \left( \frac{\xi E_{SN}}{10^{51} \text{ erg}} \right) \left( \frac{r}{1 \text{ kpc}} \right)^{-2} \left( \frac{n}{1 \text{ cm}^{-3}} \right) \text{ cm}^{-2} \text{ s}^{-1} \quad (1.10)$$

where  $r$  is the distance of SNR from earth,  $\xi$  is the fraction/efficiency of the total energy of the supernova explosion  $E_{SN}$  transferred to the cosmic ray particles and  $n$  is the average ambient matter density around the remnant. This is twice the corresponding  $\nu_e$  flux. The above expression is essentially obtained from that given by Drury et al. [26] for gamma rays. Anchordoqui et al. (2009) [162] have estimated neutrino flux for all flavor produced in hadronic proton–nucleon interaction in SNR using parametrization method and is given by

$$\frac{dF_\nu}{d(\ln E_\nu)}(> 1 \text{ TeV}) \approx 10^{-11} \left( \frac{W}{10^{50} \text{ erg}} \right) \left( \frac{r}{1 \text{ kpc}} \right)^{-2} \left( \frac{n}{1 \text{ cm}^{-3}} \right) \text{ cm}^{-2} \text{ s}^{-1} \quad (1.11)$$

where  $W$  is the total energy the cosmic ray particles gained from the supernova explosion energy. Recently Mandelartz & Becker Tjus (2015) [163] estimated high-energy neutrino spectra from 21 Galactic supernova remnants (SNRs) which are derived from gamma-ray measurements in the GeV–TeV range and find that only the strongest sources, i.e. G40.5-0.5 in the north and Vela Junior in the south could be detected as single point source by IceCube and KM3NeT respectively.

**Pulsars** are thought to be efficient neutrino emitter if charged hadrons are accelerated to 1 PeV near the surface of a young neutron star [32]. As suggested by Link & Burgio (2005) [32], the accelerated protons will scatter with the neutron star’s radiation field produce charged pions that immediately decay to neutrinos (beamed) with energies of  $\sim 50$  TeV that could produce pulsars as the brightest neutrino sources at these energies and expected neutrino flux is same as in equation 1.9. Bednarek & Protheroe (1997) [164] suggested that accelerated heavy nuclei in a Pulsar Wind Nebulae (PWNs) can photodisintegrate in collisions with soft photons produced in the pulsar’s outer gap and inject energetic neutrons that decay into protons. The neutrons decay to protons which accumulate inside the

nebula and produce neutrinos and gamma rays in collisions with the matter in the nebula. Amato et al. (2003) [165] estimated the neutrino flux from the Crab Nebula assuming accelerated hadronic components interact with the matter inside the nebula. The authors predict a few to several neutrino events in a 1 km<sup>2</sup> detector per year from the Crab Nebula. Bednarek (2003) [166] estimated the spectra of neutrinos from the interaction of nuclei inside the nebulae such as Crab Nebula (PSR 0531+21), the Vela SNR (PSR 0833-45), G 343.1-2.3 (PSR 1706-44), MSH15-52 (PSR 1509-58), 3C 58 (PSR J0205+6449), and CTB80 (PSR 1951+32) and show that only the Crab Nebula can produce neutrino event rate above the sensitivity limit of the 1 km<sup>2</sup> neutrino detector, considering that nuclei take most of the rotational energy lost by the pulsar. S. Nagataki (2004) [167] proposed another model that the neutrinos and gamma rays may be generated from the decay of charged and neutral pions in the interactions between high-energy cosmic rays themselves in the nebula flow and found that neutrinos should be detected by km<sup>2</sup> neutrino detectors such as AMANDA and IceCube if the amplitude of the magnetic field at the pole of the pulsar is  $B = 10^{12}$  G and the period of the pulsar is  $P = 1$  ms.

**Active Galactic Nuclei (AGN)** have long been considered as potential sources for high-energy neutrino production as they are the most powerful gamma ray emitters in the known Universe [168]. Stecker et al. (1991) [168] predict the production of neutrino flux from the cores of AGNs, i.e. from the accretion disk region through the collisions of ultra-relativistic protons with the intense photon fields in AGN. Nellen et al. (1993) [169] proposed that protons accelerated in the jet diffuse back to the accretion disk and initiate hadronic cascades through pp interactions. Various models have been proposed so far suggesting that neutrinos come either from the jet, and/or from the accretion disk and/or is scattered around the jet in the broad line region (e.g. Mannheim 1995 [170], Halzen & Zas 1997 [171], Bednarek & Protheroe 1999 [172], Atoyan & Dermer 2001 [36], Mücke & Protheroe 2001 [173], Mücke et al. 2003 [174], Murase et al. 2014 [175], Padovani et al. 2015 [176]). For example, Mannheim 1995 [170] calculated the diffuse background of high-energy neutrinos produced in the jets of radio-loud AGNs and found that the maximum neutrino energy reaches about 10 EeV. Most of the authors predict that neutrino spectra usually flatten below  $\sim$ PeV energies due to the threshold of the pion production in photo-hadronic collisions. As the observed shape of the neutrino spectrum follows a power law type between  $\sim$ 10 TeV and a few PeV, such models have some difficulty in explain the spectra [177].

The models which involve proton-proton interactions, seems to be more plausible neutrino production modeling (e.g. Nellen et al. 1993 [169], Beall & Bednarek 1999 [178], Schuster et al. 2002 [179], Becker Tjus et al. 2014 [181], Kimura et al. 2015 [180]) of the IceCube observations. For example, Becker Tjus et al. (2014) [181] assume two scenarios for the neutrino production, i.e. the interaction of accelerated protons with the matter of knots in the inner jets of FR-I galaxies and in the lobes of FR-II galaxies. The author concludes that only first scenario can explain the IceCube results as the second scenario requires a few orders of magnitude larger column density of the matter than expected density ( $\sim 10^{24\pm 1} \text{ cm}^{-2}$ ) in the radio lobes. Recently Bednarek (2016) [177] proposed a model that the relativistic nuclei can be accelerated in the re-connection regions in the jet and/or at the jet boundary layer, and they disintegrate in collisions with the accretion disk radiation producing relativistic neutrons. These neutrons make a cascade in the dense accretion disk and hence neutrinos and produce multi-TeV neutrinos in consistency with the IceCube observations.

**Gamma Ray Bursts (GRBs)** have been proposed as possible sources of high-energy neutrinos that are associated with high-energy cosmic-rays [182]. It is generally assumed that neutrinos are produced in photomeson interactions in GRBs. Two influential models for neutrino emission from the burst were proposed by Waxman and Bahcall [182, 183] and Guetta et al. [184] assuming neutrinos to be produced in coincidence with the prompt gamma-ray emission. However, IceCube observations for GRB neutrinos [185] have ruled out these models as observed upper limit on the flux of energetic neutrinos associated with GRBs is found at least a factor of 3.7 below the predictions. Recently, Hümmer et al. [186] revised the GRB fireball model which reduces the expected neutrino flux by about one order of magnitude than previous one and the spectrum shifts to higher energies. The authors have also concluded that the baryonic loading of the fireballs is an important control parameter for the emission of cosmic rays and it can be constrained significantly with the full-scale experiment after about ten years [186]. During other phases of GRBs, high-energy neutrinos are also predicted to be emitted. For instance, Razzaque et al. (2003) [187] predict neutrinos from shock accelerated protons in preburst jets of the stellar progenitor. Again a model of neutrino production has been also proposed by Waxman and Bahcall (2000) [188] during the afterglow phase, and they predict that such neutrinos may be detectable with recent neutrino telescope like IceCube, ANTARES etc.

## 1.5.2 Experiments

In the year of 1960, Moisei Markov was the first who proposed to install detectors deep in a lake or a sea to detect neutrinos with the help of Cherenkov radiation produced by the charged particles, created by neutrinos when they interact with nuclei in the water or ice [189]. The directions of the charged particles strongly correlate with those of the primary neutrinos. The first extraterrestrial neutrinos (in the MeV energy range) apart from the solar neutrino signal are detected from supernova SN1987A by Koshiba and collaborators in the year of 1987 [190].

**Baikal** [191] was the first neutrino telescope operating underwater after the pioneering experience made by the DUMAND Collaboration off-shore Hawaii Island. In Baikal Neutrino Telescope (NT), the detectors are deployed between 1000 and 1100 m depth in the water of Lake Baikal (Siberia). During winter, when a thick ice cap of about 1 meter is formed over the lake, deployment and recovery operations are carried out. In 1993, the telescope was NT-36 with 36 PMTs at first deployment stage but it was upgraded to Baikal NT-200 which is an umbrella-like array with a 72 m height and a diameter of 43 m in 1998 and it takes data since then [191]. The telescope NT-200 was upgraded to NT-200+ by installing 3 additional strings, has been in operation since April 2005 [191].

A new idea to utilize transparent deep polar ice as a detection medium instead of deploying the detector under water was first proposed by Francis Halzen and John Learned in 1988 [192]. **AMANDA** (The Antarctic Muon And Neutrino Detector Array), a first detector of this concept is installed near the Amundsen-Scott station at the geographical South Pole in 2000 [193]. The final detector configuration, AMANDA-II was consists of 677 Optical Modules (OMs) arranged in 19 strings and run for seven years but total exposure time of 3.8 years considering maintenance periods and acquisition system dead time. In 2007, the observatory was incorporated into IceCube observatory and AMANDA was decommissioned in May 2009 [193].

**IceCube** neutrino observatory [194], the first (& so far the only) 1 km<sup>3</sup> Cherenkov neutrino telescope is contracted in the ice near the geographic South Pole on the basis of the success of the AMANDA detector and currently under operation. In its complete configuration, IceCube consists of a total of 5160 optical sensors in 86 strings deployed between 1450 m and 2450 m depth below the surface and contraction is finished in December 2010 [194]. There are 8 strings arrayed in the

center to form a denser formation referred to as DeepCore and other strings form a triangular grid with a spacing of 125 m [194].

### 1.5.3 Observational results

Atmospheric neutrinos constitute the most important background to searches for cosmic neutrinos [195]. Baikal Collaboration detected 372 upward-going neutrino candidates from the analysis of the 5-year sample (1008 days live time) which is in good agreement with Monte Carlo simulations of atmospheric neutrinos that give 385 neutrino events to be detected in a corresponding lifetime [195].

Since 2000, AMANDA-II has been successfully recording about 1,000 neutrino events per year [196]. Using a sample of 6595 up-going muon tracks collected by AMANDA-II during 2000–2006, a search for point sources of high energy astrophysical neutrinos was performed by looking for excess of events from the directions of 26 pre-selected objects. But these neutrino events are found to be coming predominantly from atmospheric neutrinos with primary energy 100 GeV to 8 TeV and hence the search of this sample reveals no indications of a neutrino point source [197]. The search stringent an average upper limit of  $E^2\Phi_{\nu_\mu+\nu_\tau} \leq 5.2 \times 10^{-11} \text{ TeV cm}^{-2} \text{ s}^{-1}$  on the sum of  $\nu_\mu$  and  $\nu_\tau$  fluxes (assumed equal) over the energy range from 1.9 TeV to 2.5 PeV from extraterrestrial point sources in the northern sky as measured with AMANDA over seven years [197].

For IceCube experiment there are two kinds of dominant backgrounds – atmospheric muons and neutrinos produced in atmospheric air shower. As the Earth screens out muons from the Northern Hemisphere, neutrinos are only a background for Southern Hemisphere [198]. On the other hand, dominant atmospheric neutrino background can only be distinguished from astrophysical neutrinos by their energy spectrum as acceleration mechanisms for astrophysical objects are expected to produce a spectral index of 2 to 2.5 whereas observed atmospheric neutrino spectrum follows a power-law of  $\sim E^{-3.7}$  [198].

#### 1.5.3.1 Diffuse Astrophysical Neutrino Flux

There are three methods used to identify astrophysical neutrinos by IceCube: high energy starting-events (HESE), muon tracks and cascades [198]. One of

which exclusively identifies neutrinos considering only events starting within the detector fiducial volume and a thin outer ice layer of the detector acts as an active veto to reject incoming cosmic ray air shower muons, called the high energy starting-events (HESE) [198]. This veto method is sensitive to neutrinos of all flavors from all directions in the sky including both secondary showers, produced by electron and tau neutrinos in neutral current interactions of neutrinos of all flavors, and muon tracks, produced in muon neutrino charged-current interactions [199]. An active veto method was rapidly developed to find more high energy starting events (HESE) after two events having energy 1.040 PeV and 1.140 PeV were found using IceCube data collected between May 2010 and May 2012 [194]. With the veto method, IceCube collaboration recently reported 54 neutrino events with energies lying between 27 TeV and 2 PeV with expected  $12.6 \pm 5.1$  atmospheric muons and  $9.0^{+8.0}_{-2.2}$  atmospheric neutrinos by performing an analysis on 4 years of data [194, 199]. Their detected signal has  $6.5\sigma$  significance in excess over the expected flux of atmospheric neutrinos in this energy range and the flavour composition of the flux is consistent with  $\nu_e : \nu_\mu : \nu_\tau \sim 1 : 1 : 1$  as expected for a flux originating in cosmic sources [200]. The best fit all-flavor flux assuming an unbroken power law for astrophysical neutrinos using all 54 events is  $\frac{d\Phi}{dE} = (2.2 \pm 0.7) \times 10^{-18} \left(\frac{E}{100 \text{ TeV}}\right)^{-2.58 \pm 0.25} \text{ GeV}^{-1} \text{ cm}^{-2} \text{ s}^{-1} \text{ sr}^{-1}$  which is valid in the energy range 27 TeV to 2 PeV [201]. This measured distribution of neutrinos corresponds to no significant local excess in the sky and consistent with isotropy at the Earth surface. A test for galactic plane clustering was also performed and p-value of 7% is found about a Galactic width of  $2.5^\circ$  around the Galactic plane whereas a variable galactic width scan resulted in a p-value 2.5% where the arrival direction of neutrino with the smallest p-value defines a hot-spot in sky map showing the biggest deviation from background expectation [198]. Few clustering of events near our galactic center has been seen but this is statistically insignificant [198].

Another strategy of neutrino searching focuses on the observation of muon tracks passing through the detection volume produced in interaction of muon neutrinos primarily outside the detector and the Earth is used as a filter to remove the huge background of cosmic-ray muons [194]. Using the Earth as a filter in six years of data with the muon track event sample, a flux of neutrinos is identified with  $6\sigma$  significance in excess over the expected flux of atmospheric neutrinos at energies beyond 100 TeV [194]. At energies between 191 TeV and 8.3 PeV, the astrophysical neutrino  $\nu_\mu + \bar{\nu}_\mu$  flux is well described by a best fit unbroken power law

as  $\frac{d\Phi}{dE} = (0.9^{+0.30}_{-0.27}) \times 10^{-18} \left(\frac{E}{100 \text{ TeV}}\right)^{-2.13 \pm 0.13} \text{ GeV}^{-1} \text{ cm}^{-2} \text{ s}^{-1} \text{ sr}^{-1}$  which is consistent with the all-sky all flavor flux measured from starting events [194, 202]. There are 29 events with reconstructed muon energy greater than 200 TeV, with the highest energy of  $2.6 \pm 0.3$  PeV found out from the total 352,294 events, but their arrival direction did not show any spatial/timing clustering and neither correlated with any gamma ray source catalogs considered [203].

In the cascade channel, all the energy of a neutrino is deposited near the vertex due to neutral current interactions or charged current interactions from electron and tau neutrinos and thus have much better energy resolution than tracks, but at the cost of relatively poor angular resolution. A total of 172 events were observed with energies between 10 TeV and 1 PeV in an analysis of the first two years of data. The astrophysical component is also well demonstrated by a power-law as  $\frac{d\Phi}{dE} = (2.3^{+0.7}_{-0.6}) \times 10^{-18} \left(\frac{E}{100 \text{ TeV}}\right)^{-2.67 \pm 0.13} \text{ GeV}^{-1} \text{ cm}^{-2} \text{ s}^{-1} \text{ sr}^{-1}$  with a significance of  $4.7\sigma$  over atmospheric neutrino background [204].

A global spectral analysis was done by combining the results of these analyses along with the results of 3 other diffuse analysis and it is found that the all-flavor spectrum with neutrino energies between 25 TeV and 2.8 PeV is well described by an unbroken power law with a flux of  $6.7^{+1.1}_{-1.2} \times 10^{-18} \text{ GeV}^{-1} \text{ cm}^{-2} \text{ s}^{-1} \text{ sr}^{-1}$  at 100 TeV and a best-fit spectral index  $2.50 \pm 0.09$  assuming the astrophysical neutrino flux to be isotropic with equal flavors at Earth [202].

### 1.5.3.2 Search for Neutrino Point Sources

IceCube has better sensitivity to identify point sources with angular resolution  $< 1^\circ$  in the northern sky using through-going track-like events which are predominantly atmospheric muon neutrinos [199]. Using 7 years data over the period from 2008 to 2015 with over 700,000 track-like events, a search for all sky time-independent clustering of astrophysical neutrinos did not find any significant steady point like emission. IceCube collaboration performed both untriggered fine grid full sky scan and correlated observed neutrinos to pre-selected 74 gamma ray sources. Results for some selected such sources with the smaller p-values are shown in Table 1.3. The blazar 1ES 1959+650 is found to be one of the most significant source in northern sky having the pre-trial p-value of 1.8% in northern sky [205]. The Pulsar wind nebula HESS J1616-508 in the southern sky is another most significant source with best fit pre-trial p-value of 0.22% but no

significant clustering of high-energy events is observed for all cases [205]. Results usually stringent upper limits on steady astrophysical point source flux are set on the level of  $E_\nu^2 \frac{d\Phi}{dE_\nu} \sim 10^{-12} \text{ TeV}^{-1} \text{ cm}^{-2} \text{ s}^{-1}$  and data are consistent with the background neutrino flux [205].

TABLE 1.3: Searches for neutrino emission from predefined candidate sources with IceCube. The type, common name, and equatorial coordinates of the objects with selected p-values and 90% C.L. upper limits on  $\nu_\mu + \bar{\nu}_\mu$  fluxes  $E_\nu^2 \frac{d\Phi}{dE_\nu} \leq \Phi_{90} \times 10^{-12} \text{ TeV}^{-1} \text{ cm}^{-2} \text{ s}^{-1}$  are shown for each object [205].

Type	Source	$\alpha(^{\circ})$	$\delta(^{\circ})$	p-value	$\Phi_{90}$
BL Lac	PKS 2005-489	302.37	-48.82	0.071	13.45
	1ES 1959+650	300.00	65.15	0.018	2.36
	Mrk 421	166.11	38.21	0.32	0.94
	Mrk 501	253.47	39.76	0.18	1.15
Flat-spectrum radio quasar	PKS 1406-076	212.24	-7.87	0.053	1.65
	3C 273	187.28	2.05	0.25	0.59
PNWs	Crab Nebula	83.63	22.01	0.34	0.68
	HESS J1616-508	243.78	-51.40	0.0022	19.37
SNRs	Cas A	350.81	58.81	0.14	1.49
	IC443	94.21	22.50	0.22	0.83
	TYCHO	6.36	64.18	0.27	1.23
Massive star cluster	HESS J1614-518	243.58	-51.82	0.0058	18.33
Not identified	MGRO J1908+06	286.98	6.27	0.025	0.99

Other searches which use a stacked maximum likelihood method, correlate neutrinos to a same category of sources to probe the scenario of distributed weak sources [199]. Using such analysis, a recent search for steady astrophysical neutrino emission was performed for 862 blazars, detected in GeV gamma rays but no significant excess was observed, constraining that less than 20% of the observed astrophysical neutrino flux could have come from blazars [199].

To investigate GRBs as high energy neutrino emitter, an analysis incorporating 4 years of muon track events and 506 observed Northern Hemisphere bursts was performed but no correlation more significant than expected from background was found [206]. A similar result was found with a 3 years search using the cascade channel correlated with 807 GRBs from the whole sky [207]. These analyses set a limit on the neutrino flux which disfavor some parameter space for the neutrino emission theories from GRBs and constraining that less than 1% of the observed astrophysical neutrino flux could have come from GRBs [199].

## 1.6 Objectives of the thesis

Supernova remnants appears the only viable class of galactic source of cosmic rays up to the knee or even up to the ankle energy. As mentioned already the SNRs fulfill two important requirements as candidate source of cosmic rays – the energy budget of cosmic rays and viable acceleration (DSA) mechanism. Some aspects are, however, not yet settled. The maximum attainable energy is one of the key unsettled issues concerning the SNR model of Cosmic ray origin. The maximum energy that can be attained by a Cosmic ray particle in an ordinary SNR when the remnant is passing through a medium of density  $N_H \text{ cm}^{-3}$  is [208–211]

$$E_{max} \simeq 4 \times 10^5 Z \left( \frac{E_{SN}}{10^{51} \text{ erg}} \right)^{1/2} \left( \frac{M_{ej}}{10M_{\odot}} \right)^{-1/6} \left( \frac{N_H}{3 \times 10^{-3} \text{ cm}^{-3}} \right)^{-1/3} \left( \frac{B_o}{3\mu G} \right) \text{ GeV} \quad (1.12)$$

which for proton primary is falling short even of the knee of the Cosmic ray energy spectrum (around 3 PeV) by about one order of magnitude. The problem is, however, somewhat alleviated by the fact that the effective magnetic field strength at the shock can be amplified due to growth of magnetic waves induced by accelerated Cosmic rays. With the amplified field, the maximum energy achieved in SNR possibly can reach even as far as the ankle.

The maximum energy that a charged particle can gain by diffusive shock acceleration is proportional to  $Z$ . The knee (at around 3 PeV) of the cosmic ray energy spectrum is usually assigned as the maximum energy that protons can have under diffusive shock acceleration in SNRs. Under the SNR origin of cosmic rays framework, the mass composition of cosmic rays will be heavier beyond the knee if the knee is a proton knee. The primary cosmic rays are studied directly through satellite or balloon borne detectors only up to few hundreds TeV, beyond which direct methods become inefficient due to a sharp decrease in the flux of primary particles, and instead an indirect method, through the observation of cosmic ray extensive air showers (EAS), which are cascades of secondary particles produced by interactions of cosmic ray particles with atmospheric nuclei, has to be adopted. Several EAS measurements have been carried out to determine the mass composition of cosmic rays in the PeV energy region and above, but the conclusions of

different experiments on primary mass composition in the PeV energy region are not unequivocal, which is mainly due to the weak mass resolution of the measured EAS observables (Haungs 2011) [14]. So it will be very useful if some alternative technique is found for determination of cosmic ray composition in PeV energy range.

The SNR origin model of cosmic rays has received some supports from the TeV gamma ray observations. If the cosmic rays are accelerated in SNRs, hadronic interactions of cosmic ray nuclei with the ambient matter/radiation will produce neutral and charged pions which in turn decay into gamma rays and neutrinos respectively. Several SNRs have been detected by the modern gamma-ray observatories in TeV and GeV energies in the past fifteen years or so (Aharonian 2013 [212] and references therein). But the evidence is only supportive but not conclusive as leptonic mechanisms such as inverse Compton scattering of thermal/ambient photons with energetic electrons also may lead to the TeV gamma-ray emission from the SNRs. Detection of high energy neutrinos is believed to lead the unambiguous identification of the acceleration sites of hadronic cosmic rays.

Under the context the objectives of the present thesis are

- i) to explore the consequences of the maximum attainable energy of cosmic rays in SNR as  $Z$  times the knee energy, where  $Z$  is the atomic number, as may be achievable under amplified magnetic field scenarios, on the secondary gamma-ray spectrum of young supernova remnants.
- ii) to investigate theoretically the implication of maximum attainable energy of cosmic rays to PeV energies in supernova remnants on high energy gamma rays and neutrinos from molecular clouds proximity to the SNR and whether ongoing/near future experiments of gamma rays/neutrinos can resolve the maximum energy issue or not by observing high energy gamma rays/neutrinos from molecular clouds around the SNR.
- iii) to analyze the fluxes of high energy gamma rays and neutrinos produced in interaction of high energy cosmic rays with solar radiation and coronal matter as a cosmic ray mass spectrometric technique
- iv) To critically examine the conventional idea that high energy neutrinos are dominantly originated only in hadronic processes by comparing the flux of leptonic originated and hadronic originated high energy neutrinos from a viable cosmic ray source.